Chapter 5

Polymeric Micelles of LSF- LA Conjugate

1. Introduction

In the previous chapter, we discussed the detailed synthesis of self-assembling conjugate of LSF (LSF-LA). The synthesized LSF-LA conjugate self-assembled into micelles (LSF-LA SM) resulting in a drastic improvement in the physicochemical properties as well as the PK profile of LSF along with a significant decrease in its conversion rate to the inactive metabolite, PTX as compared to the free drug.[1] In addition to this, the conjugate exhibited improved efficacy in animal model of T1DM at a reduced dose of 15 mg/kg, once daily in comparison to the free drug administered at 25mg/kg, twice daily to provide a therapeutic response albeit, a weaker one as compared to LSF-LA SM. Nevertheless, when LSF-LA SM was administered orally in vivo, it failed to exhibit oral bioavailability (24.46 % in compare to free LSF 22.43 %) because of easily cleavable ester linkage between LSF and LA; which underwent a rapid cleavage in GIT before it could reach into the systemic circulation. As an alternate to this, to enhance the oral bioavailability of LSF and further to decrease its interconversion into PTX, we developed its polymeric micellar formulation which could protect the LSF-LA ester linkage from degradation in the GIT environment and provide sustained release of LSF.

In the light of the above mentioned facts, in the present work, our objective was to develop an orally active, polymeric nanoformulation of LSF-LA conjugate and reduce interconversion of LSF to PTX. LSF-LA conjugate was encapsulated into micelles of an *in-house* synthesized amphiphilic block polymer methoxypoly(ethylene glycol)-b-poly(carbonate-co-L-lactide) block copolymer (mPEG-b-P(CB-co-LA). The polymeric micelles of LSF-LA were tested for their stability upon storage at 2-4 °C and RT (25 °C) and ability to release free LSF in plasma. Further evaluation in cell culture studies in rat insulinoma cells, MIN-6 for their cytotoxicity, β-cell protective effect and insulin secretory ability under inflammatory conditions, PBMCs proliferation and cellular uptake were carried

out. This formulation exhibited a drastic improvement in the oral PK profile of LSF along with a significant decrease in its conversion to the inactive metabolite, PTX as compared to the free drug and LSF-LA SM resulting in significantly improved oral bioavailability (oral bioavailability of free LSF *vs.* LSF-LA SM *vs.* LSF-LA mPEG-b-P(CB-co-LA) micelles (LSF-LA PLM) was found to be 22.43, 24.46 and 74.86% respectively in rats). Apart from improvement in oral PK profile, LSF-LA PLM formulation demonstrated equivalent therapeutic efficacy both by oral route as well as parenteral route (i.p.) of administration in STZ induced T1D rat model which was further supported by analysis of various biochemical parameters in different animal groups and confirmed by histopathological and immunohistochemical analysis of diabetic rat pancreatic tissues.

2. Materials and Methods

2.1. Materials, reagents and experimental animals

LSF (purity ≥98%) was synthesized *in house* as per *chapter 2*. LA (purity ≥99%, HPLC) was obtained Hi-Media Laboratories (Mumbai, INDIA). STZ, 3-Isobutyl-1-methylxanthine (IBMX; ≥99%, HPLC; Internal standard), MTT, D-glucose stannous 2-ethylhexanoate ($Sn(Oct)_2$), 2,2-bis(hydroxymethyl) propionic acid (BHMP), 2,2- methoxy poly(ethylene glycol) (mPEG, Mn 5000) and DL-Lactide were purchased from Sigma Aldrich (St. Louis, MO). Triphosgene, benzyl bromide, pyridine, potassium hydroxide and ammonium chloride were procured from SRL pvt. Ltd. (INDIA). DMEM, FBS and TrypLE were obtained from Invitrogen (USA); BSA, DMSO (Molecular biology grade) and PBS pH 7.4 were purchased from Hi-Media Laboratories. ELISA kits for TNF-α and IFN-γ (ELISA MAX^{TM}) were obtained from BioLegend (USA). Recombinant TNF-α, IL-1β and IFN-γ were obtained from Invitrogen (MD, USA). CFSE staining assay kit (CellTrace™), Ficoll-Paque and PHA were obtained from Thermo Fisher (USA). Accucheck Active Glucometer was purchased from Roche Diabetes Care India Pvt. Ltd. (Mumbai, INDIA). All the kits for determination of

biochemical parameters were purchased from Coral clinical systems (INDIA). All other chemicals and reagents were of analytical grade and used as obtained. Antibodies used in immunohistochemistry including CD4 Rabbit mAb (Cat# 25229); signal stain IHC boost reagent (anti-rabbit; Cat# 8114) and anti-mouse IgG (H+L) antibody (Cat# 7076) were purchased form Cell signaling technologies and CD8a Mouse mAb (OX-8 Cat# 550298) was procured from BD Pharmingen®. MIN-6 cell line was procured from NCCS, Pune (INDIA). Wistar rats (male; 8–10 weeks, 200–220 g) were procured from Central Animal Facility, BITS-PILANI (Pilani, India). All animal experiments were performed as per CPCSEA guidelines and according to protocols approved by Institutional Animal Ethics committee (IAEC) (Animal testing protocol # IAEC/RES/23/26; Central animal facility (CAF), BITS-Pilani).

2.2. Synthesis and characterization of mPEG-poly(carbonate-co-lactide)[mPEG-b-P(CB-co-LA)]

To improve the delivery, pharmacokinetics and stability of LSF-LA conjugate in comparison to free LSF and LSF-LA SM, amphiphilic polymer with carbonate blocks (5-methyl-5-benzyloxycarbonyl-1,3-dioxane-2-one; MBC) was synthesized as reported earlier by our group[2] with modification in the preparation method. Instead of the previously reported method (130°C for 24 h), microwave synthesizer (Monowave 300; Anton paar GmbH, Austria) was employed to facilitate the polymerization reaction and the reaction time was reduced from 24 h to 45 min along with improved yield of polymer.

For synthesis of $mPEG_{114}$-b-P(CB_{25}-co-LA_{50}), first MBC monomer was synthesized and purified as reported earlier [3,4] followed by ring-opening polymerization reaction of mPEG, DL-lactide, and MBC using stannous 2-ethylhexanoate (10 mol% relative to mPEG) as a catalyst at 130°C for 45 min in microwave synthesizer. The copolymer so obtained was dissolved in chloroform and purified using chilled isopropyl alcohol (twice)

and diethyl ether (once). Polymer characterization was carried out using the following techniques:

2.2.1. Nuclear Magnetic Resonance (NMR)

^{1}H NMR spectra were recorded on a Bruker (400 MHz) using deuterated chloroform ($CDCl_3$) as a solvent. The chemical shifts were calibrated using tetramethylsilane as an internal reference (0.00 ppm) and given in parts per million. Further, number average molecular weight and the units of lactic acid and MBC present in the final polymer were calculated using mPEG peak integral value (456 protons) as standard.

2.2.2. Gel permeation chromatography (GPC)

The number average molecular weight and PDI of synthesized polymer was determined by a Waters GPC system equipped with HPLC pump (Waters 515), autosampler (Waters 2707), GPC column (HR4 Styragel® Column, HR 4, 10^4Å, 5 μm, 7.8 mm × 300 mm, 5K – 600 kDa, column oven and a differential refractive index detector (Waters 2414). $CHCl_3$ (HPLC grade) was used as an eluent at a flow rate of 1 mL/min. A series of narrow polystyrene standards (3.27 to 120.0 kDa) were used for calibration of molecular weights.

2.2.3. CMC

Determination of CMC was carried out following the same procedure as reported in previous chapter (Chapter 4; section 2.5). Briefly, mPEG-b-P(CB-co-LA) at various dilutions (5.0 × 10-5 mg/ mL-1.0 mg/mL) was mixed with pyrene (6 x 10-7 M) in different test tubes and incubated at room temperature (RT) for 48 h to ensure the solubilization of pyrene in aqueous phase. The emission spectra of the solution were recorded at 320-450 nm keeping emission wavelength at 390 nm. A plot was constructed between I3/I1 ratio versus logarithm of mPEG-b-P(CB-co-LA) concentration wherein, the I3 and I1 values

were determined from the peak intensities at the wavelengths of 337 nm and 333 nm. The CMC value of mPEG-b-P(CB-co-LA) was determined from the intersection of the best-fit lines.

2.2.4. Aggregation number (Nagg) determination

As reported in previous chapter, **chapter 4**, Stern-Volmer equation was employed to determine the aggregation number of the LSF-LA PLM (**Chapter 4; section 2.6**).[5,6] Steady-state fluorescence quenching method was used to determine the mean aggregation number in polymeric micelles by using a fluorescence spectrophotometer (Shimadzu RF-5301). Pyrene and cetylpyridinium chloride (CPC) were used as probe and quencher respectively. For fluorescence measurements, stock solutions of pyrene (2×10^{-6} M) in PLM at 10 times the CMC value and pyrene + CPC (2.8×10^{-2} M) in PLM micellar solution at 10 times the CMC value were prepared. Appropriate volumes of these two solutions were then mixed to vary the CPC concentration from 0 to 1.54×10^{-3} M. By exciting the samples at 318 nm, emission spectra of pyrene were obtained and the emission was measured in the range of 320–450 nm. The emission peak at 376 nm was considered for calculating the micellar aggregation number.

2.3. Formulation development and characterization of LSF-LA conjugate loaded PLM

LSF-LA PLM was prepared by thin-film hydration method. LSF-LA conjugate (20 mg) and polymer (180 mg) in DCM were transferred into a round bottom flask, thin film was prepared by solvent evaporation under vacuum, followed by reconstitution of the film with water with stirring for 30 min. Resulting micellar formulation was sonicated for 1 min under cold conditions and characterized for size, zeta potential, encapsulation and loading efficiency. Blank PLM (BLK) formulation was also prepared by similar method without LSF-LA conjugate.

2.3.1. Particle size, zeta potential and morphology determination

Measured using Zetasizer Nano-ZS (Malvern Instrument Ltd., UK) with a helium laser at 633 nm and the scattering angle was fixed at 173°. Morphology of the developed formulation was studied using high resolution transmission electron microscopy (HR-TEM; JEM 2100, Jeol Ltd., Japan).

2.3.2. Drug loading (DL) and Entrapment efficiency (EE)

% DL and EE of LSF-LA conjugate in LSF-LA PLM were estimated using previously reported HPLC-PDA method. For drug loading calculation, formulation was lyophilized and drug content was analyzed by HPLC. Practical drug loading (**Equation 1**) and EE were calculated using following formulae (**Equation 2**):

$$\text{Drug loading } (\%\ \text{DL}) = \frac{W_0}{Wt} \times 100 \qquad \textbf{Equation 1}$$

$$\text{Encapsulation efficiency } (\%\ \text{EE}) = \frac{W_0}{W1} \times 100 \qquad \textbf{Equation 2}$$

where, W_0 is the weight of drug entrapped in micelles, W_t is weight of lyophilized micelles and W_1 is the amount of drug initially added in the system.

2.4. Stability of LSF-LA PLM formulation

In Simulated biological fluids: Stability of drugs/dosage forms in simulated biological fluids indicates the likelihood of oral bioavailability. Stability of different formulations (LSF-LA PLM and LSF-LA SM) was determined in simulated gastric fluid (SGF, pH 1.2), simulated intestinal fluid (SIF, pH 6.8) and PBS (pH 7.4). SGF and SIF without enzymes were prepared as per USP. A stock solution of LSF-LA SM/LSF-LA PLM (500 µg/mL) was added to SGF, SIF and PBS (n=3) separately and incubated at 37 °C and 100 rpm in shaking water bath. An aliquot of sample (200 µL; without replacement of media) was collected at each time point (0, 10, 20, 30, 45, 60, 90 and 120 min for SGF; 0, 10, 20, 30, 45, 60, 90, 120, 180 and 240 min for SIF and 0, 10, 20, 30, 45 min, 1, 2, 4, 6, 8 ,12 and 24 h for PBS)

followed by quenching of the sample with ice cold acetonitrile (800 µL), vortexing and centrifugation, then the supernatant was collected and LSF-LA conjugate in samples was analyzed by HPLC. The graph between % LSF-LA remaining intact in the medium and time was plotted considering LSF-LA at initial time point (0 min) as 100%.

***At different storage temperatures*:** Stability of LSF-LA PLM upon dispersion in water was assessed at two different storage temperatures: a) at RT (25 °C) and, b) at 4 °C for a period of 30 days by determining particle size and PDI of the LSF-LA PLM at a time interval of 3 days upto 30 days.

2.5. Ex-vivo release study of LSF-LA PLM in rat plasma

LSF-LA PLM (10 mg) containing LSF-LA conjugate (~1 mg equivalent of LSF) was added to rat plasma (1 ml) and kept at 37 ℃ for 72 h. At pre-determined time points, 200 µL of sample (without replacement of media) was withdrawn to which 50 µL of internal standard (IBMX, 2 µg/mL) and 2 mL of DCM were added. The resulting mixture was vortexed for 5 min and centrifuged at 3500 rpm for 15 min at 4℃, after which the supernatant was transferred into a fresh tube and evaporated to dryness under nitrogen. Dried samples were reconstituted in 100 µL of mobile phase and analyzed by HPLC (Shimadzu, Japan) using our previously reported method.

2.6. Cell culture based studies for LSF-LA PLM

To evaluate the efficacy of LSF-LA PLM conjugate in hyperglycemic/diabetic conditions, mouse insulinoma cells, MIN-6 were used. Cells were grown in RPMI media supplemented with 10% FBS and 1% antibiotic solution and grown at 37 °C in a humidified atmosphere containing 5% CO_2. For treatments, LSF-LA and LA were dissolved in cell culture grade DMSO and the highest used concentration of DMSO was kept as control (0.1% v/v).

2.6.1. Inflammation mediated β-cell death and decrease in insulin secretion

MIN6 cells (5×10^3/well) were exposed to a cocktail of pro-inflammatory cytokines (TNF-α; 10 ng/mL, IL-1β; 5 ng/mL and IFN-γ; 100 ng/mL) to induce inflammation.[7] To these cells, along with LSF-LA PLM and controls (Free LSF, LA, LSF-LA SM, BLK) at ~20 μM in the presence of cytokines and incubated for 48 h. Thereafter, the cells were evaluated for their viability by MTT assay and insulin secreting ability by a static incubation method using basal (3.33 mM) and stimulatory glucose (33.33 mM) concentrations prepared in Krebs-Ringer bicarbonate HEPES buffer (pH 7.4). After 1h of incubation, supernatants were collected and analyzed for insulin using commercially available ELISA kit. Cytotoxicity assay for all the treatments (at ~20μM) was also performed in MIN6 cells in the absence of any cytokines to check toxicity of formulations in absence of inflammatory conditions.

2.6.2. PBMCs proliferation and activation

PBMCs were freshly isolated from mouse blood using Ficoll-Paque density gradient method. These cells were then exposed to PHA (3 μg/mL, mitogen activator) in the presence of LSF-LA PLM (~20 μM) and suitable controls as free LSF, LA, LSF-LA SM (all at ~ 20 μM) and BLK. After 96 h, the supernatants were evaluated for PBMCs proliferation using CFSC staining assay kit as per manufacturer's instructions using flow cytometry with a 488 nm excitation laser. [8] The extent of cell activation was also determined by measuring the level of inflammatory cytokines, TNF-α and IFN-γ in the conditioned medium of PBMCs using ELISA kits.

2.6.3. Cellular uptake of LSF-LA PLM

MIN6 cells were incubated with LSF-LA PLM and LSF-LA SM (~20 μM to LSF) for 6 h keeping LSF (20 μM) and untreated cells as controls. After 6 h incubation, LSF-LA and free LSF were quantified in cultural supernatants using previously reported HPLC method.

2.7. Pharmacokinetics of free LSF, LSF-LA SM and LSF-LA PLM

The PK studies of LSF, LSF-LA SM and LSF-LA PLM were performed on Wistar rats (200-220 g). LSF (solution in water), LSF-LA SM and LSF-LA PLM were administered orally at the dose of 10 mg/kg (~LSF) with maximum dosing volume of 1 mL to each rat with overnight fasting (n=4). For oral bioavailability determination of LSF in comparison to LSF-LA, these were also administered intravenously at 10 mg/kg dose. After dosing, blood samples were collected at pre-determined time points up to 36 h. Plasma concentration-time profiles were plotted and analyzed for various pharmacokinetic parameters by non-compartmental model using Phoenix 2.1 WinNonlin (Pharsight corporation, USA). Since LSF is known to interconvert to PTX, plasma levels of PTX were also assessed in all the PK studies of LSF and its formulations to understand the rate and extent of interconversion of LSF to PTX.

2.8. In vivo efficacy studies in T1DM model

Diabetes was induced in the male wistar rats weighing 180-220 g. Animals were maintained under standard environmental conditions and provided with feed and water *ad libitum*. Initially, for one week (prior to the experimentation), all the animals were fed on normal pellet diet (NPD). Animals were injected with single high dose of STZ (45 mg/kg, i.p.) dissolved in sodium citrate buffer (0.01 M, pH 4.5) while the respective control rats received the vehicle (citrate buffer (pH 4.5) only. After 72 h of STZ injection, fasting glucose levels were measured, animals showing plasma glucose levels >250 mg/dl were considered diabetic. Thereafter, glucose and insulin levels of the experimental animals were checked throughout the study by tail bleeding method.

2.8.1. Experimental design

Animals were randomly divided into eight different groups as shown in **Table 5.1.**

Treatment was started on 3rd day after confirming the diabetic conditions. For treatment, LSF and LA (in 0.5 % *w/v* tween 80) were administered as solutions prepared in water for injection at a dose of 15 mg/kg, once daily. LSF-LA SM IP (by i.p. route), LSF-LA PLM IP (by i.p. route) and LSF-LA PLM ORAL (by oral route) were given at a dose equivalent to 15 mg/kg

Table 5.1
Experimental groups for efficacy studies in STZ induced T1DM model.

S. No.	Experimental groups
1	Normal Control (NC)
2	Diabetic Control (DC)
3	PLM blank formulation (BLK)
4	Free Lisofylline (LSF)
5	Free Linoleic acid (LA)
6	LSF-LA SM via IP route (LSF-LA SM IP)
7	LSF-LA PLM via IP route
8	LSF-LA PLM via Oral route

of LSF (~ 30 mg/kg of LSF-LA) once daily. Treatment was continued for 3 weeks and fasting glucose levels were measured twice weekly by tail bleeding method using Accu-Check active glucometer. After 3 weeks, the levels of insulin and inflammatory cytokines, TNF-α and IFN-γ were measured in serum using commercially available ELISA kits.

2.8.2. Evaluation of blood and serum biochemical parameters

In diabetes, there are significant changes in serum protein and lipid profile as well as liver and kidney functions before and after treatment with hypoglycemic agents. To assess the effect of LSF-LA PLM on lipid and protein profile of animals, serum protein, cholesterol and triglycerides levels were measured. For liver and kidney function, SGPT, SGOT, serum urea,

uric acid were also measured. All biochemical parameters were measured after 3 weeks of study period using commercially available kits (Coral diagnostics, INDIA).

2.8.3. Histopathology and immunohistochemical (IHC) analysis

After 3 weeks of treatment, animals were euthanized and pancreata were isolated and fixed in 4% paraformaldehyde solution. Tissues were then processed for paraffin embedding, subsequent serial sectioning, and staining with hematoxylin/eosin (H&E) to allow the assessment of pancreatic islet morphology in the studied groups. IHC analysis was also performed in pancreas for expression of CD4+ and CD8+ T-cells as per standard protocol. After immunostaining, the sections were lightly counterstained with hematoxylin and observed under a light microscope. Primary antibodies, CD4 Rabbit mAb and CD8a Mouse mAb were optimized at dilution of 1:400 and 1:20 respectively. Signal stain IHC boost reagent and anti-mouse IgG (H+L) antibody were used as secondary antibody at a dilution of 1:1 (3-4 drops) and 1:500 respectively.

3. Results

3.1. Characterization of mPEG-b-P(CB-co-LA) polymer

To deliver LSF-LA conjugate, mPEG-b-P(CB-co-LA) copolymer was synthesized and characterized using ^{1}H NMR and GPC. ^{1}H NMR showed the presence of 26 units of MBC monomer and 50 units of lactic acid in the copolymer with an overall molecular weight of 15,168 Da (**Figure 5.1)** and the molecular weight determined by GPC was found to be 13,047 Da **(Figure 5.2**). As shown in **Figure 5.3A and 5.3B**, synthesized polymer showed a CMC of 5.95 µg/mL and an aggregation number (N_{agg}) of 14.82 at 10 times the CMC value.

3.2. Formulation characterization

LSF-LA conjugate loaded PLM prepared by thin-film hydration method exhibited self-assembly demonstrating a particle size of 149.3 nm (PDI: 0.209) and zeta potential -7.23 mV respectively (**Figure 5.3C**). Entrapment efficiency of LSF-LA in PLM was found to be 75 ±

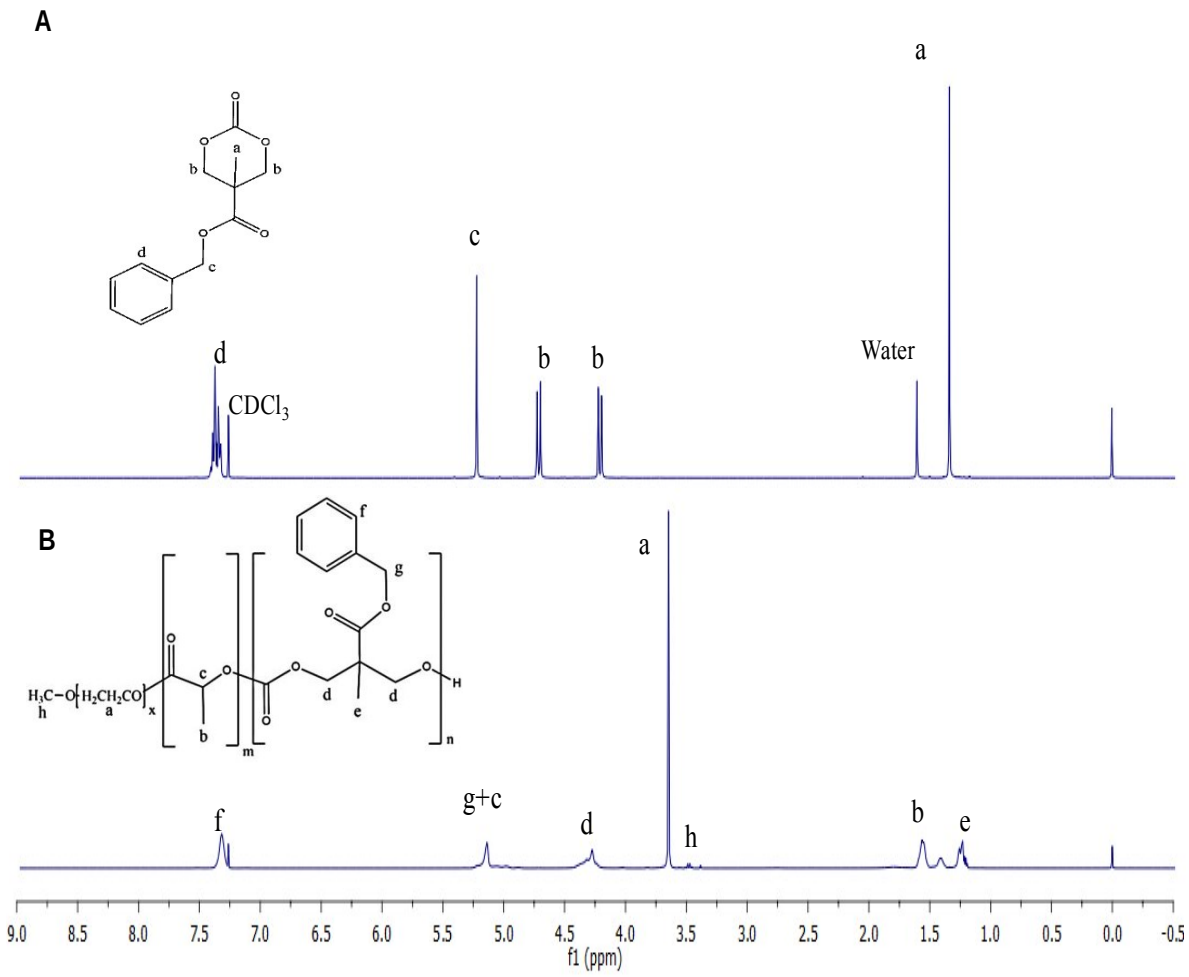

Figure 5.1 ^{1}H NMR of *in house* synthesized mPEG$_{114}$-b-P(CB$_{25}$-co-LA$_{50}$) polymer (A) 5-methyl-5-benzyloxycarbonyl-1,3-dioxane-2-one (MBC) monomer and (B) mPEG$_{114}$-b-P(CB$_{25}$-co-LA$_{50}$) polymer respectively

4.12% with a practical drug loading of 9.29 ± 1.16%. **Figure 5.3D** shows TEM image of LSF-LA PLM confirming the spherical morphology of the micelles.

3.3. *Stability study of LSF-LA PLM*

Stability studies of LSF-LA PLM at 4 and 25 °C (RT), revealed no significant change in the size and PDI of LSF-LA PLM at both the temperatures **(Figure 5.3E)**. As shown in **Figure 5.4 (A, B and C**), LSF-LA conjugate (free) was not found to be stable in SGF (only 22.95 ± 1.16% intact LSF-LA after 2 hr) and SIF (only 17.73 ± 6.37% intact LSF-LA after 4 hr) even in the absence of enzyme) and exhibited a half -life of 1.3 hr and 1.12 hr for SGF

and SIF respectively but was found to be stable in PBS (102.29 ± 4.20% of LSF-LA was found to be intact even after 24 hr). However, LSF-LA PLM showed stability in all the

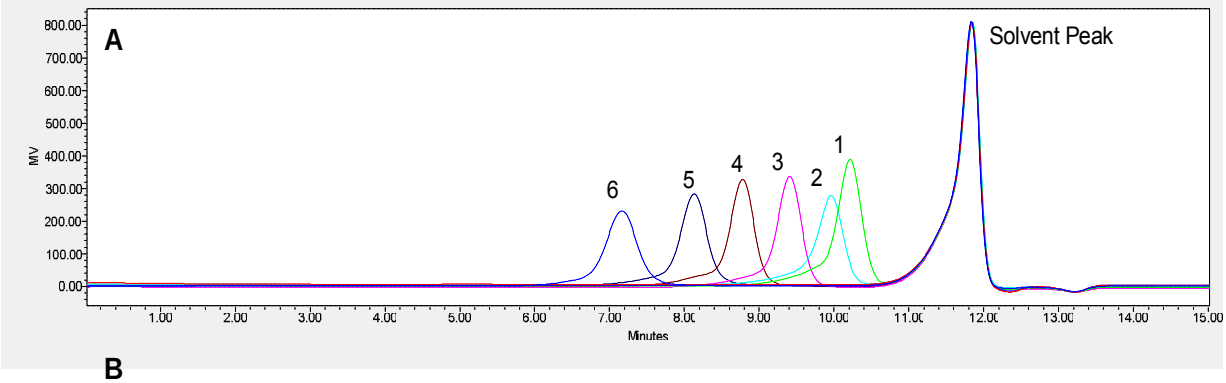

C

S.no.	Standard Molecular Weight (in KDa)		
	Mn	Mw	Mp
1.	3.26	3.46	3.47
2.	5.27	5.61	5.44
3.	12.00	12.50	12.60
4.	26.60	27.50	28.00
5.	50.00	51.50	54.00
6.	120.00	125.00	130.00

D

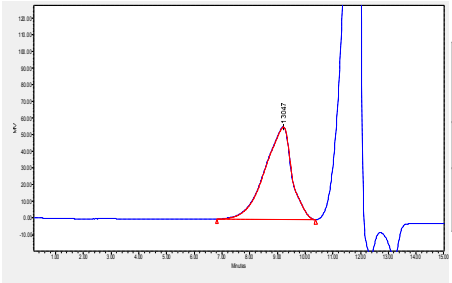

E

Molecular weight (Da) of $mPEG_{114}$-b-P(CB_{26}-co-LA_{50})	
^{1}H NMR	GPC
15168	13047

Figure 5.2 GPC analysis of $mPEG_{114}$-b-P(CB_{25}-co-LA_{50}) polymer. (A) and (B) Overlay chromatograms of polystyrene standards and calibration curve respectively; (C) M.W. of polystyrene standards for generating calibration curve; (D) and (E) GPC Chromatogram of $mPEG_{114}$-b-P(CB_{26}-co-LA_{50}) polymer and calculated molecular weight respectively

media, including SGF, SIF and PBS wherein, 112.61 ± 4.26% of LSF-LA conjugate could be detected intact in case of PLM after 2 hr of incubation in SGF; 76.05 ± 7.13% after 4 hr of incubation in SIF and 101.61 ± 5.15% after 24 hr in PBS. This, data clearly indicated the feasibility of administering LSF-LA PLM by oral route.

3.4. Ex-vivo release study of LSF-LA PLM in rat plasma

As shown in **Figure 5.4D**, LSF LA PLM released LSF-LA conjugate into the plasma which further underwent hydrolysis to release free LSF which is then available to elicit its

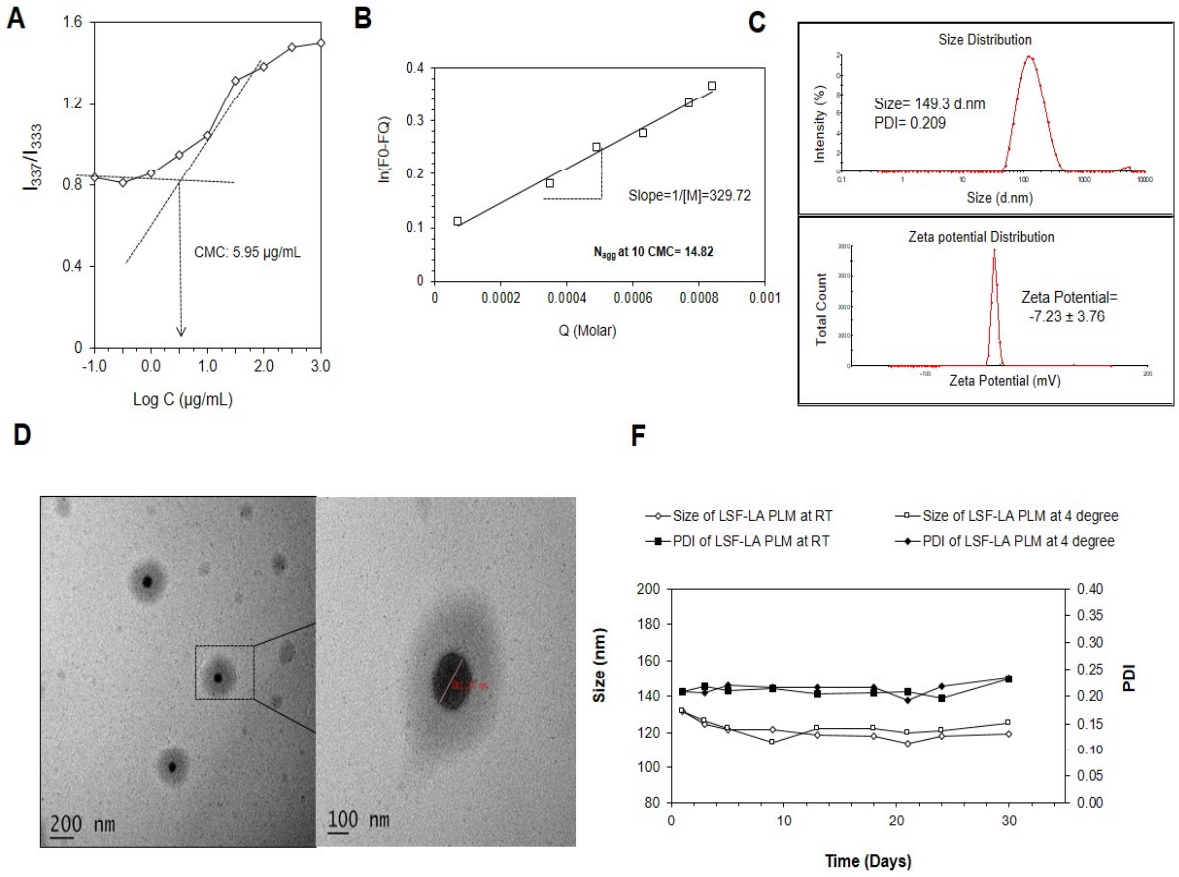

Figure 5.3. Characterization of blank and LSF-LA loaded mPEG-b-P(CB-co-LA) micelles (PLM). (A) CMC of PLM determined by fluorescence spectroscopy using pyrene as fluorescent probe (CMC: 5.95 µg/mL); (B) micellar aggregation number of PLM at 10*CMC value determined by pyrene as fluorescent probe and cetylpyridinium chloride (CPC) as a quencher (N_{agg}: 14.82); (C) particle size and zeta potential distribution of LSF-LA PLM; (D) particle morphology of LSF-LA PLM by HR-TEM analysis and, (E) LSF-LA PLM stability at room temperature (RT) and 4°C for 30 days: particle Size and PDI analysis

therapeutic effect. After 48 h of incubation in plasma, 68.17 ± 1.63% of free LSF was released from LSF-LA PLM. Mass balance studies were carried out to detect the remaining

amount of un-hydrolysed LSF-LA conjugate in PLM under alkaline conditions however,

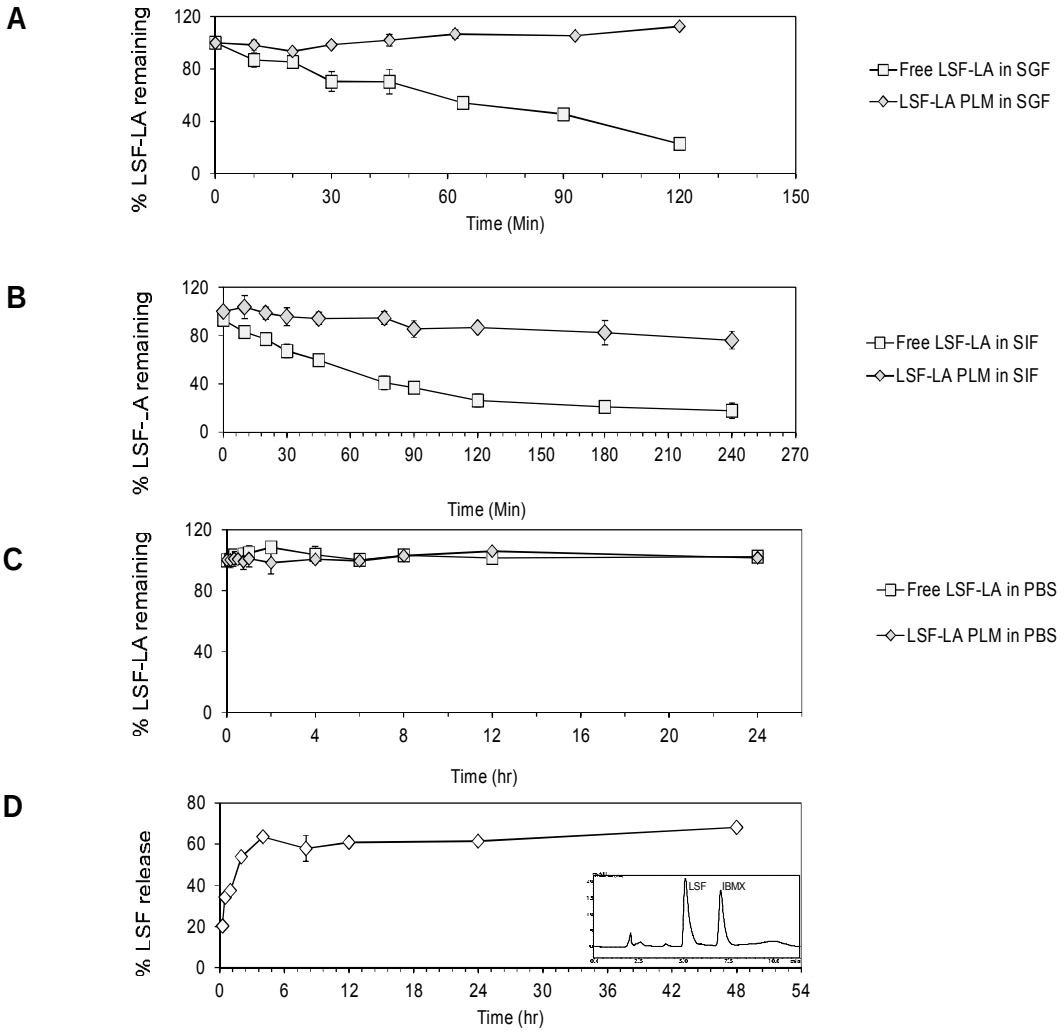

Figure 5.4. Stability of LSF-LA PLM in comparison to LSF-LA conjugate in different physiological fluids, (A) Simulated gastric fluid (SGF; pH 1.2); (B) simulated intestinal fluid (SIF; pH 6.8); (C) PBS (pH 7.4) and, (D) *ex-vivo* release of LSF from LSF-LA PLM in rat plasma and representative chromatogram for 1 h sample.

owing to the degradation of LSF under alkaline conditions, remaining LSF could not be detected.

3.5. Cell culture based evaluation of LSF-LA PLM

The major objective of these experiments was to evaluate if the activity/ potency of LSF-LA conjugate remains intact after encapsulation into the PLM that is, if any processes and excipients used during formulation development have affected the anti-diabetic activity

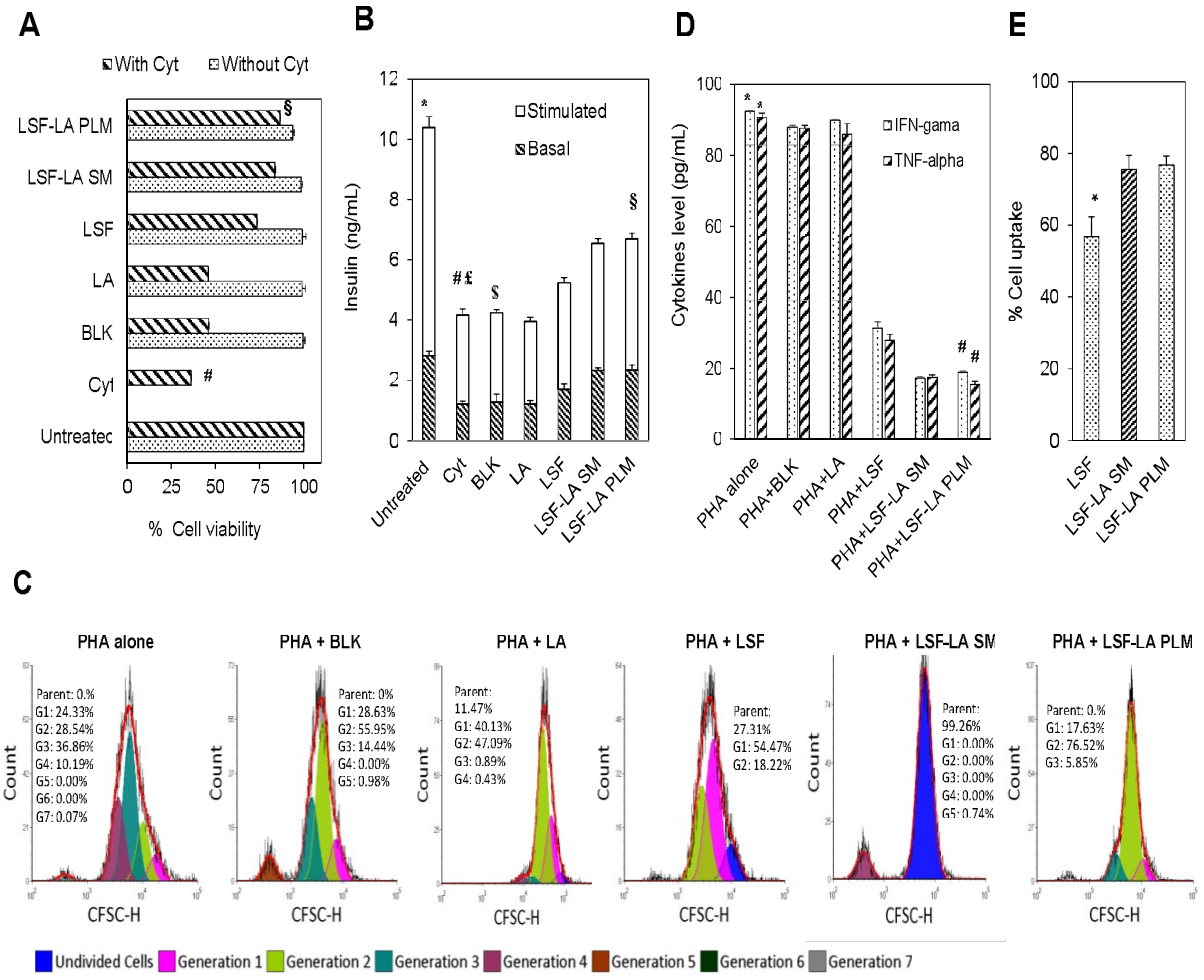

Figure 5.5. In-vitro cell culture evaluation of LSF-LA PLM (~20μM) in MIN6 cells (A) Cytotoxicity evaluation (MTT assay) in the presence and absence of cytokines (TNF-α, IL-1β and IFN-γ). $^{\#}$Cyt *vs.* all; §LSF-LA PLM *vs.* LSF and LA ($^{\#\S}p < 0.001$); (B) Basal and stimulated insulin levels after inflammatory challenge *Untreated *vs.* all: $^{\#}$Cyt *vs.* LSF, LSF-LA SM and LSF-LA PLM; $^{\$}$BLK *vs.* LSF-LA SM and LSF-LA PLM: §LSF-LA PLM *vs.* LSF and LA ($^{*\#\S}P < 0.001$); (C) Spontaneous proliferation of PBMCs (after stimulation with PHA) studied by CFSE staining and analyzed by FlowJo software; (D) IFN-γ and TNF-α (pg/mL) levels in the conditioned media of PBMCs stimulated with PHA. *PHA stimulated PBMCs *vs.* LSF and LSF-LA SM and PLM; $^{\#}$LSF-LA PLM *vs.* LSF ($^{*\#}p<0.001$); and (E) Cell uptake study using HPLC. *LSF *vs.* both ($^{*}p< 0.05$)

of the conjugate in any way.

3.5.1. Inflammation mediated β-cell death and decrease in insulin secretion

It is well known that release of pro-inflammatory cytokines during diabetes causes the death of β-cells and thus severely compromises both basal as well as post-prandial insulin levels. Cytotoxicity assay of LSF-LA PLM and blank micelles (BLK) revealed that these were non-toxic towards insulin secreting pancreatic beta cells, MIN-6 in absence of cytokines. However, in the presence of a cocktail of cytokines (TNF-α, IL-1β and IFN-γ), cell viability was reduced to ~36.28% (**Figure 5.5A)** along with a drastic reduction in the level of insulin when compared to normal cells (without cytokines) (**Figure 5.5B)**. However, upon incubation of the cells, with free LSF, LSF-LA SM and LSF-LA PLM (~20 μM) (in the presence of cytokines), a sharp increase in cell viability upto 73.21, 82.63 and 86.68% respectively was observed. Further, the basal insulin level which dropped to 1.12 ng/mL in the presence of cytokines showed an increase to 1.58, 2.27 and 2.34 ng/mL in the presence of LSF, LSF-LA SM and LSF-LA PLM respectively. LSF-LA PLM showed a statistically significant increase in the viability of β -cells and insulin levels in comparison to free LSF but similar to that of LSF-LA SM indicating similar *in-vitro* therapeutic efficacy of LSF-LA after formulating into polymeric micelles.

3.5.2. PBMCs proliferation and activation

Presence of LSF and LSF-LA SM/PLM in the growth medium of PBMCs caused a significant reduction in the proliferation of PBMCs even in the presence of a mitogen stimulator (**Figure 5.5C**) which otherwise exhibited spontaneous proliferation upto 7 generations in the presence of PHA alone. Levels of inflammatory cytokines, IFN- γ and TNF-α were also determined in the conditioned media of PBMCs after stimulation with PHA. As shown in **Figure 5.5D**, LA and BLK treated cells did not exhibit any significant difference in IFN- γ and TNF-α level as compared to PHA only stimulated cells. However,

LSF-LA SM and LSF-LA PLM treatment revealed a significant reduction in the levels of cytokines in PHA stimulated cultures ($p< 0.001$) signifying retention of therapeutic efficacy of LSF during/after formulation development and also the ability of LSF-LA PLM to impair the activation of adaptive immune system in T1D.

3.5.3. Cellular uptake studies for LSF-LA PLM

LSF-LA PLM revealed a significantly higher uptake into the cells (76.78±2.46 %) after incubation for 6 h in comparison to the free LSF group (56.86 ± 9.26 %) but not statistically significant from LSF-LA SM (75.48 ± 4.01 %) (**Figure 5.5E**).

3.6. Pharmacokinetics studies

Interconversion of LSF to PTX was confirmed when PTX was found in the plasma upon i.v. administration of LSF and its formulations (**Figure 5.6A).** As shown in **Table 5.2,** LSF-LA PLM significantly improved the oral pharmacokinetic parameters of LSF. Upon oral administration, LSF-LA PLM showed a half-life of 2.09 ± 0.05 h which was 3.4 folds higher than that free LSF (0.61 ± 0.06 h). Thus, LSF-LA PLM increased MRT of LSF (from 0.81 to 2.41 h). Further, AUC_{0-t} for LSF-LA PLM was found to be 4252.69 ng.h/mL which is 3 times higher than AUC_{0-t} observed in LSF-LA SM (1389.73 ng.h/mL) after oral administration. Interestingly, while LSF-LA SM exhibited a low oral bioavailability of 24.46%, it got significantly improved to 74.86% upon administration of LSF-LA PLM (**Figure 5.6B**). This indicated the possibility of designing an orally viable delivery system for LSF which otherwise has a negligible oral bioavailability.

As shown in **Figure 5.6**, plasma concentration of PTX was much lower upon administration of LSF-LA PLM in comparison to LSF and LSF-LA SM PK (**Figure 5.6A and 5.6C**) which indicated that there was a significant decrease in the rate and extent of LSF-PTX *in vivo* interconversion upon administering LSF as a self-assembling conjugate, LSF-LA

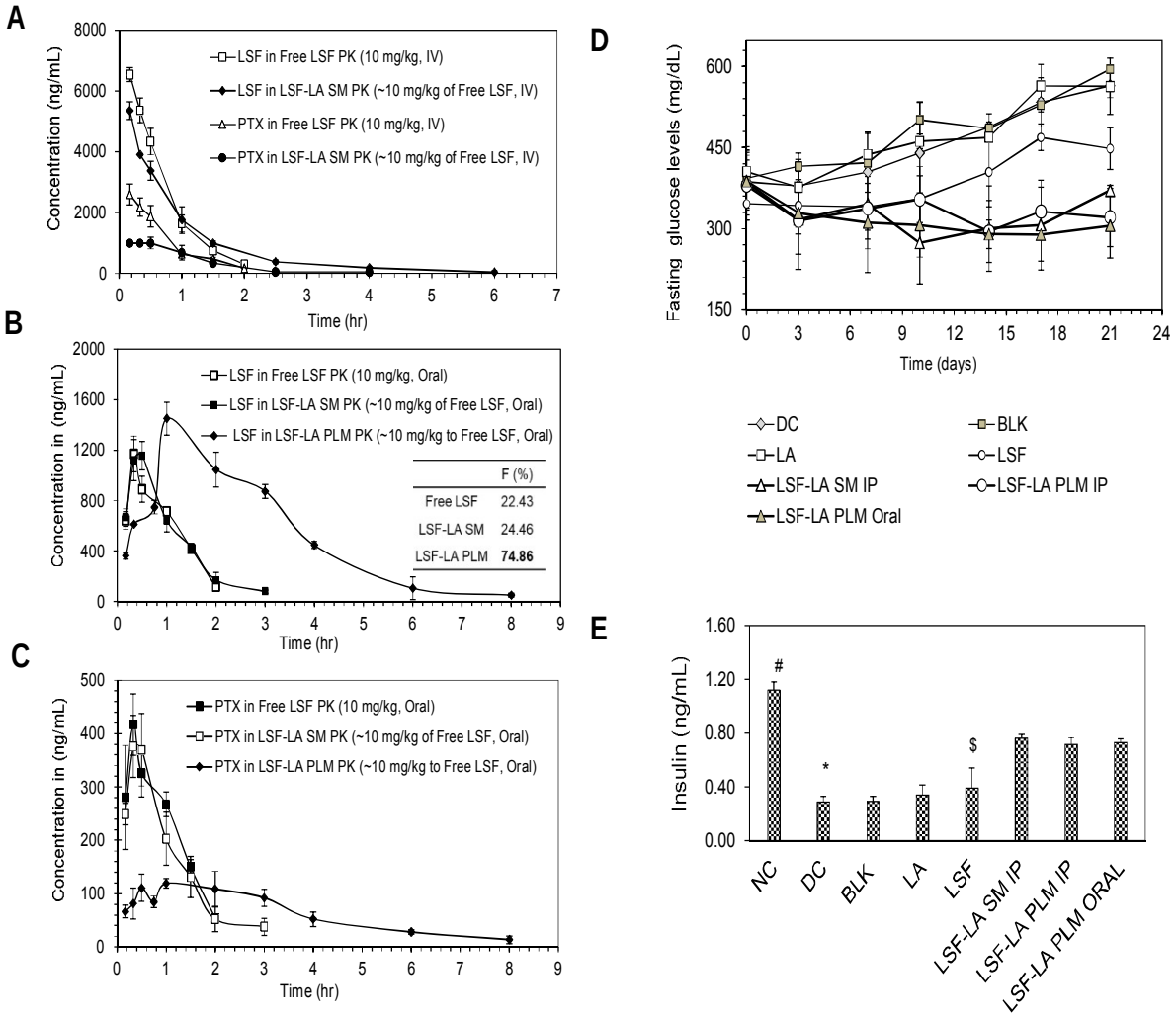

Figure 5.6. *In-vivo* PK and PD studies of LSF-LA PLM: Pharmacokinetic studies (~10 mg/kg dose) in normal rats (Mean ± SEM, N=4); (A) LSF and PTX plasma concentration-time profiles obtained after i.v. administration of free LSF and LSF-LA SM in rats, (B) LSF plasma concentration-time profiles obtained from free LSF, LSF-LA SM and LSF-LA PLM after oral administration, F: Oral bioavailability; (C) PTX plasma concentration-time profiles obtained from free LSF, LSF-LA SM and LSF-LA PLM after oral administration. Anti-diabetic effect of LSF-LA PLM in STZ induced T1D model: (D) and (E) Fasting blood glucose levels and serum insulin levels respectively in STZ induced diabetic rats after 3 weeks of treatment with LSF-LA PLM via IP and oral route with suitable controls †. $^{\#}$NC *vs* all groups; *DC *vs* LSF-LA groups; $^{\$}$LSF *vs* LSF-LA groups; $^{\#*\$}P<0.001$. †NC, DC, BLK, LA, LSF and LSF-LA SM IP

Table 5.2A.
The non-compartmental pharmacokinetic parameters for free LSF and LSF-LA SM (IV) PK.

	Free LSF; IV (Mean ± SEM)		**LSF-LA SM; IV (**Mean ± SEM)	
Parameters	LSF	PTX	LSF	PTX
Co (ng/mL)	7781.23 ± 434.35	4881.70 ± 929.97	7354.68 ± 532.15	1060.68 ± 87.73
$t_{1/2}$ (h)	0.39 ± 0.03	0.48 ± 0.04	0.96 ± 0.01	0.70 ± 0.08
AUC0-last (ng.h/mL)	5289.77 ± 332.91	2510.72 ± 179.52	5680.53 ± 461.19	1438.40 ± 228.66
AUC0-∞ (ng.h/mL)	5450.27 ± 366.96	2632.88 ± 158.85	5794.56 ± 471.25	1492.91 ± 253.14
AUMC0-last (ng.h/mL)	2663.41 ± 278.63	1312.27 ± 67.94	5718.25 ± 513.71	1266.88 ± 288.85
AUMC0-∞ (ng.h/mL)	3080.74 ± 400.24	1645.22 ± 19.99	6560.78 ± 587.14	1547.63 ± 417.61
MRT (h)	0.50 ± 0.03	0.53 ± 0.02	1.00 ± 0.01	0.85 ± 0.07

Table 5.2B.
The non-compartmental pharmacokinetic parameters for Free LSF (Oral) PK

	Free LSF; Oral (Mean ± SEM)	
Parameters	**LSF**	**PTX**
C_{max} (ng/mL)	1138.64 ± 134.72	504.36 ± 38.44
$t_{1/2}$ (h)	0.61 ± 0.06	0.69 ± 0.07
Ke (1/h)	0.94 ± 0.06	1.04 ± 0.11
AUC0-last (ng.h/mL)	1186.75 ± 70.40	491.12 ± 22.86
AUC0-∞ (ng.h/mL)	1321.69 ± 63.34	547.20 ± 18.29
AUMC0-last (ng.h/mL)	962.17 ± 35.82	379.06 ± 8.68
AUMC0-∞ (ng.h/mL)	1379.63 ± 27.71	549.76 ± 37.80
MRT (h)	0.81 ± 0.02	0.77 ± 0.02

Table 5.2C.
The non-compartmental pharmacokinetic parameters for LSF-LA SM and LSF-LA PLM (Oral) PK

	LSF-LA SM; Oral (Mean ± SEM)		**LSF-LA PLM; Oral (**Mean ± SEM)	
Parameters	LSF	PTX	LSF	PTX
C_{max} (ng/mL)	1168.40 ± 89.73	409.55 ± 50.92	1449.39 ± 119.09	121.12 ± 12.30
$t_{1/2}$ (h)	0.72 ± 0.03	0.67 ± 0.09	2.09 ± 0.05	2.96 ± 0.35
K_e (1/h)	0.96 ± 0.04	1.12 ± 0.18	0.33 ± 0.01	0.24 ± 0.03
AUC0-last (ng.h/mL)	1389.73 ± 111.51	406.33 ± 71.28	4252.69 ± 125.07	440.16 ± 30.75
AUC0-∞ (ng.h/mL)	1473.64 ± 124.12	471.32 ± 100.42	4409.34 ± 132.71	492.49 ± 28.78
AUMC0-last (ng.h/mL)	1273.34 ± 122.10	303.23 ± 64.17	10264.00 ± 531.25	1195.61 ± 82.78
AUMC0-∞ (ng.h/mL)	1614.18 ± 176.66	508.83 ± 167.07	11993.57 ± 568.57	1851.07 ± 172.48
MRT (h)	0.91 ± 0.02	0.72 ± 0.05	2.41 ± 0.07	2.72 ± 0.09

keeping free LSF, LA, LSF-LA SM and BLK treated diabetic animals as controls (~15 mg/kg, once daily).

which was further reduced upon encapsulating the LSF-LA conjugate in self -assembling polymeric micelles, LSF-LA PLM.

3.7. In vivo efficacy studies in STZ induced T1DM model

LSF-LA PLM was tested by IP and oral routes of administration in STZ induced T1D rat model over a 3 week time period at 15 mg/kg dose (equivalent to free LSF), once daily,

As shown in **Figure 5.6D**, a decrease in the fasting glucose levels was observed throughout the treatment period after LSF-LA PLM administration beginning from day 3 of treatment.

LSF lowered glucose levels in some rats but was unable to maintain the reduced levels compared to LSF-LA SM IP, LSF-LA PLM IP and LSF-LA PLM Oral. LSF-LA PLM IP and LSF-LA PLM oral exhibited lowered as well as stabilized blood glucose levels as compared to diabetic animals. As shown in **Figure 5.6E,** LSF-LA PLM treated group showed significantly increased level of insulin in comparison to control groups along with a drastic reduction in TNF-α and IFN-γ level (**Figure 5.7A**). LSF-LA PLM delivered by oral route exhibited similar levels of insulin and TNF-α and IFN-γ as that LSF-LA SM IP and LSF-LA PLM IP; implying similar efficacy of LSF-LA PLM by oral route of administration as that of IP.

Regarding the biochemical parameters, a change in the levels of serum cholesterol, triglycerides, SGPT (ALT), SGOT (AST), urea, uric acid and total protein was observed in the diabetic animals as compared to the normal animals. LSF-LA SM and LSF-LA PLM (by both the routes) significantly decreased the levels of serum cholesterol, triglycerides, SGPT, SGOT, urea, uric acid whereas, these treatments significantly increased the serum level of protein in comparison to NC, DC, LA, LSF and BLK treated groups (**Figure 5.7**).

3.7.1. In-vivo histology and immunohistochemical analysis

Histological examination of the H&E-stained sections of rat pancreas of diabetic group showed a significant decrease in the number of β cells of the islets of Langerhans in comparison to the control group (normal animals) wherein, the islets showed a large number of β cells (seen as hematoxylin-stained blue cells) distributed throughout the islet (**Figure 5.8**). The damage or necrosis of β cells in diabetic control group is a hallmark of diabetes. In

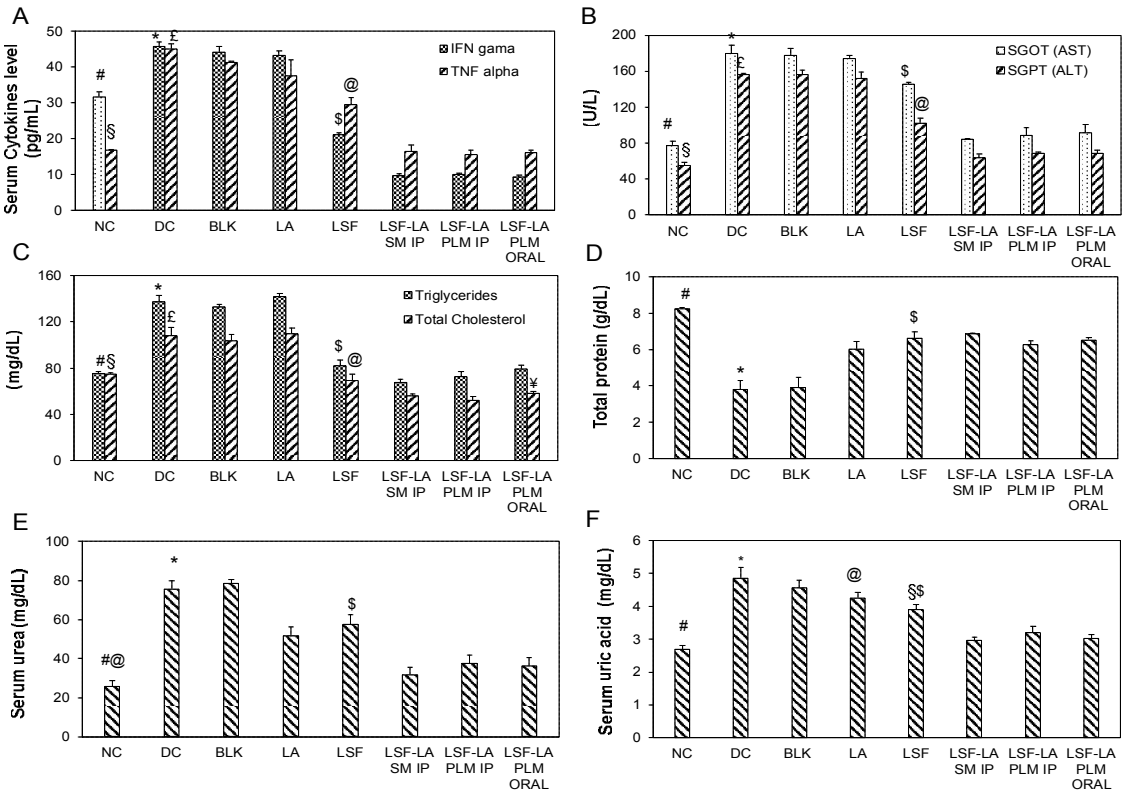

Figure 5.7. Effect of LSF-LA PLM on different biochemical parameters in STZ induced T1DM model after 21 days of treatment. (A) Serum cytokines levels (IFN-γ and TNF-α), $^{\#}$NC *vs* all groups for IFN-γ and §NC *vs* DC, BLK, LA, LSF for TNF-α: $^{*£}$DC *vs* LSF, LSF-LA groups; $^{\$@}$LSF *vs* LSF-LA groups; $^{\#*\$\S£@}$P<0.001, (B) SGOT (AST) and SGPT (ALT), $^{\#\S}$NC *vs* DC, BLK, LA, LSF; $^{*£}$DC *vs* LSF, LSF-LA groups; $^{\$@}$LSF *vs* LSF-LA groups; $^{\#*\$\S£@}$P<0.001 (C) triglycerides and total cholesterol, $^{\#}$NC *vs* DC, BLK, LA for triglycerides and §NC *vs* DC, BLK, LA, LSF-LA groups for total cholesterol; $^{*£}$DC *vs* LSF, LSF-LA groups; $^{\$@}$LSF *vs* LSF-LA SM IP and SM PLM IP; $^{¥}$LSF-LA PLM oral *vs* LSF; $^{\#*\$\S£@}$P<0.001, $^{¥}$P<0.05 (D) total protein, $^{\#}$NC *vs* all groups; *DC *vs* LSF, LA, LSF-LA groups; $^{\$}$LSF *vs* BLK, LA; $^{\#*\$}$P<0.001, (E) serum urea, $^{\#}$NC *vs* DC, BLK, LA, LSF;$^{@}$NC *vs* LSF-LA groups; *DC *vs* LSF, LA, LSF-LA groups; $^{\$}$LSF *vs* LSF-LA groups; $^{\#*\$}$P<0.001, $^{@}$P<0.05 and, (F) serum uric acid level, $^{\#}$NC *vs* DC, BLK, LA, LSF;$^{@}$LA *vs* LSF-LA groups; *DC *vs* LSF and LSF-LA groups; $^{\$}$LSF *vs* LSF-LA PLM IP; §LSF *vs* LSF-LA SM IP, LSF-LA PLM oral $^{\#*\$@}$P<0.001, $^{\$}$P<0.05

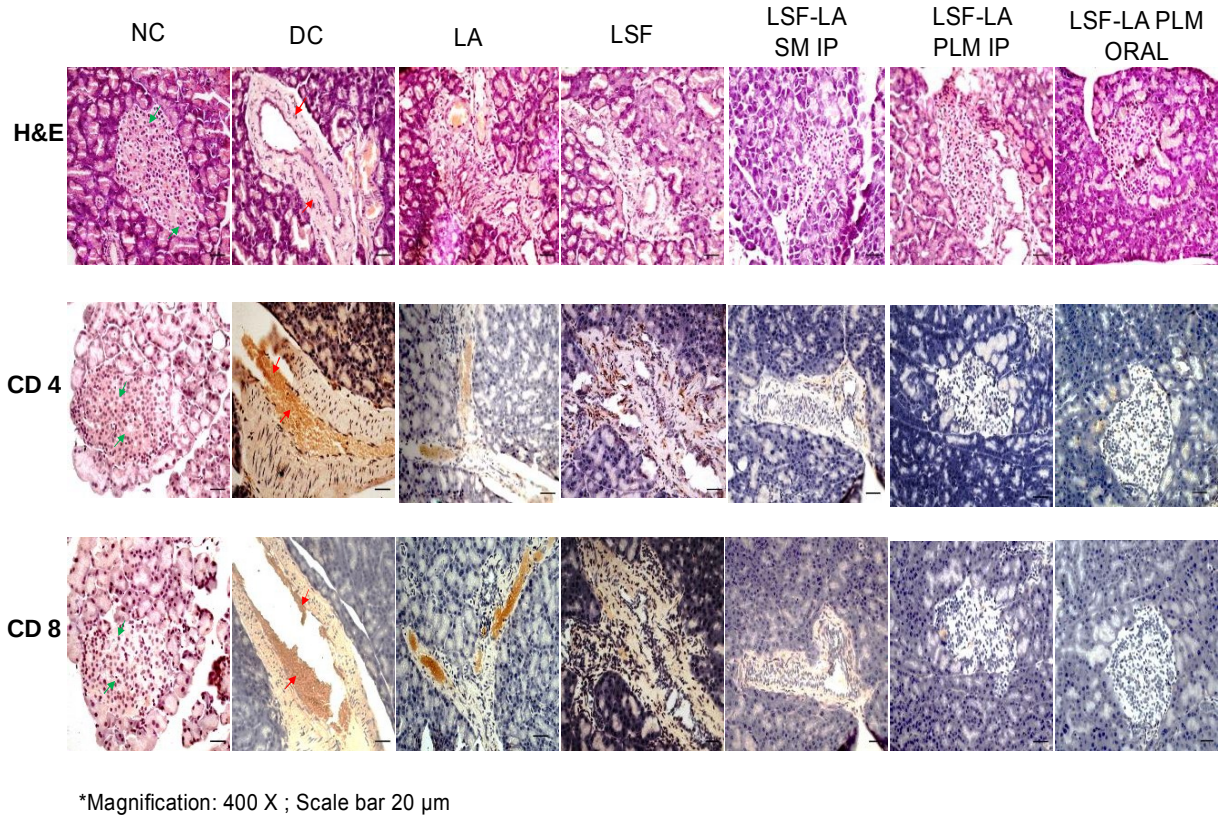

Figure 5.8. Histological and immunohistochemical analysis of pancreatic sections after 21 days of treatment: Hematoxylin-eosin staining and expression of CD4+ and CD8+ T- cells

LSF-LA micelles treated groups (LSF-LA SM and LSF-LA PLM), more number of β cells were observed along with reduced β cell fibrosis and inflammatory cell infiltration as compared to the diabetic control and LA treated groups. This also explains the higher plasma insulin levels observed at the terminal end point (21 days) in LSF-LA PLM treated group in comparison to the control groups (**Figure 5.6E**) and similar observation in *in-vitro* cell

culture experiments which revealed an increase in cell viability and insulin secretion under the inflammatory conditions upon treatment with LSF-LA PLM (**Figure 5.5C**). Further as shown in **Figure 5.8,** expression of CD4+ and CD8+ inflammatory T-cells was carried out in pancreatic sections of the experimental animals. The high numbers of CD4+ and CD8+ stained T cells in DC and LA groups were consistent with active islet β-cell destruction as revealed by H&E staining in these groups. In rats treated with LSF-LA conjugate micelles

(LSF-LA SM and PLM), CD4+ and CD8+ positive cell clusters were less prominent throughout the pancreas. Treatment with free LSF showed higher number of CD4+ and CD8+ inflammatory cells in comparison to LSF-LA micelles treated groups. Among the LSF-LA micelles treated groups, LSF-LA PLM (by both oral and IP routes) showed minimal infiltration of inflammatory T cells in comparison to LSF-LA SM.

4. Discussion

Designing a patient compliant and effective delivery system for a therapeutic molecule is a challenging task given the limitations regarding its solubility, stability, targeted release profile and pharmacokinetics.[9] One such difficult to deliver but potent molecule is LSF associated with major limitations, that make its delivery quite complicated and hence it remains a poorly explored drug. As an attempt to resolve these limitations of LSF, in this thesis, we first reported a drug-fatty acid conjugate of LSF with fatty acid LA which showed self-assembly into micelles (LSF-LA SM) and exhibited potent activity and efficacy in *in vitro* and *in vivo* experiments at a reduced dose and dosage mainly attributed to reduced interconversion of LSF to its inactive metabolite PTX by blocking free hydroxyl group in side chain of LSF. LSF-LA SM is the first reported injectable nanoformulation of LSF which made its sustained delivery possible for a variety of autoimmune disorders.[1] Considering that T1D is a chronic ailment which requires multiple injections of the anti-diabetic agent every day, parenteral route of administration is certainly not a patient friendly alternative.[10,11] LSF-LA SM, when tested by oral route of administration showed a very low bioavailability (24.46% in rat) due to the ease of cleavage of ester linkage between LSF and LA in the GIT before reaching the systemic circulation.

We designed an orally viable nano-drug delivery system for the synthesized LSF-LA conjugate to enhance its potential for clinical translation. Shielding the ester bond between LSF and LA against cleavage in GIT by encapsulating it in a polymeric carrier not only

demonstrated equivalent therapeutic activity by oral and parenteral route but also decreased the interconversion of LSF to PTX substantially (**Figure 5.6C**).

For this purpose, LSF-LA conjugate was encapsulated into an *in-house* designed self-assembling amphiphilic polymeric carrier. Among the different types of nanoparticulate formulations available, we selected polymeric micelles owing to their self-assembling nature, high encapsulation efficiency, controlled release, small size, biocompatibility and biodegradability.[12-14] Additionally, polymeric micelles show enhanced stability and resistance to drug leakage under normal physiological conditions.[15] To develop polymeric micelles of LSF-LA conjugate, we screened several polymers which could self-assemble and provide high payload. Literature suggests that hydrophilic fraction of 0.25-0.4 ($f_{\text{hydrophilic}}$) in amphiphilic copolymers enables their self-assembly or aggregation into lamellar, micellar or vesicular systems in aqueous solutions.[16,17] Primarily, we synthesized the polymeric carrier with a hydrophilic fraction of 0.3 or 30% comprising of PEG_{114} (M_n-5000) while 70% of the weight fraction was composed of hydrophobic segments consisting of lactic acid and MBC, wherein, 50 units of lactic acid and 26 units of MBC were attached to mPEG in the final polymer. Previously, M. Danquah et al. synthesized PEG-b-polyester/polycarbonate copolymer system [poly(ethylene glycol)-b-poly(carbonate-co-lactide)] using conventional technique which normally requires 130°C for 24 hr for synthesis.[4] We modified the technique to a microwave synthesizer based technique which reduced the reaction time from 24 hr to 45 min. Since our objective was to obtain a high drug loading, we varied the ratios of lactide and MBC in the final polymer without changing the weight fraction of hydrophilic and hydrophobic segments and the copolymer containing 26 units of MBC monomer and 50 units of lactic acid was selected for further studies. Self-assembling nature of the polymer was confirmed by determination of CMC value (5.95 µg/mL) and aggregation number (14.82 at 10 CMC). LSF-LA conjugate was

encapsulated into the polymer [$mPEG_{114}$-b-P(CB_{25}-co-LA_{50})] by simple film hydration method and formation of spherical micelles was confirmed by TEM (**Figure 5.3D**).

To ensure oral bioavailability of any molecule, its stability in the lumen of the GIT is important which is often compromised due to the acid mediated enzymatic degradation of the molecule in the upper gut.[18,19] This might be the reason for low oral bioavailability of our previously designed, LSF-LA SM. Hence the stability of LSF-LA PLM in GI tract was important to assess to ensure its oral bioavailability. Unlike LSF-LA which underwent substantial degradation in SGF and SIF (**Figure 5.4A and B**), LSF-LA PLM remained stable in all the simulated biological fluids (SGF, SIF and PBS at pH 1.2, 6.8 and 7.4 respectively). This might be attributed to the higher stability and shielding effect of the micellar structure in LSF-LA PLM in the acidic pH of the SGF (pH 1.2). It has been reported that the strength of the hydrogen bonds is much higher under acidic conditions which plays a key role in enabling self-assembly of the amphiphilic polymers into micelles.[20,21] However, as the pH becomes alkaline in SIF (pH 6.8), the hydrogen bonding gets weakened thus favoring the disassembly of micelles resulting in minor release of LSF-LA from LSF-LA PLM (**Figure 5.4B**). These results provided preliminary indication that the prepared $mPEG_{114}$-b-P(CB_{25}-co-LA_{50}) polymer could remain stable in the hostile environment of GIT and being nano-sized could be easily absorbed into the systemic circulation. Once into the systemic circulation, it would be able to release free LSF as revealed by the hydrolysis study of LSF-LA PLM in plasma (**Figure 5.4D**) wherein, slow and sustained release of free LSF (68.17 ± 1.63%) was observed from the nanoformulation within 48 hr. A slow rate of hydrolysis of the conjugate also indicated possibility of prolonged action and reduced rate of metabolism *in vivo* in turn reflecting the possibility of reduced dose and dosage. These results indicated that the designed system has the potential of proving to be a good carrier for oral delivery of LSF which was later validated by

pharmacokinetic and pharmacodynamic studies. However, before proceeding to *in vivo* experiments, it was necessary to ensure that the potency and efficacy of LSF in LSF-LA PLM remains similar as was seen in LSF-LA SM. To meet this objective, cell culture based evaluation was carried out which revealed that LSF-LA PLM was non-toxic to MIN-6 cells. In fact, LSF-LA PLM protected these insulin secreting cells from death under cytokine-induced inflammatory conditions and boosted their insulin release (**Figure 5.5B**) similar to that of LSF-LA SM. Cytokines (TNF-α, IL-1β and IFN-γ) are responsible for direct β -cell cytotoxic action in rodent islets which could ultimately result in pathogenesis of T1D. PBMC proliferation and cellular uptake studies also indicated similar activity of LSF-LA PLM formulation as observed with LSF-LA SM at same dose. It was evident from these results that the activity of LSF-LA PLM was intact and similar to that of LSF-LA conjugate. Although, LSF-LA PLM exhibited a significant improvement in PK parameters over LSF-LA conjugate which was clearly reflected during the pharmacodynamic studies in diabetic animals, however, cell culture studies carried out in controlled and static environment, cannot explore these advantages of LSF-LA PLM.

To prove the oral efficacy of the formulation, PK studies were conducted wherein, upon oral administration of LSF-LA SM, ester linkage present in conjugate got directly exposed to hydrolase enzymes present in GIT, resulting in the cleavage of the ester bond. So, PK parameters of orally administered LSF-LA SM did not show any significant improvement in comparison to free LSF for example, LSF-LA SM showed half-life of 0.72 h in comparison to free LSF (0.61 h). AUC was also found to be 1389.73 and 1186.75 ng.h/mL respectively for LSF-LA SM and free LSF. So, based on oral PK data of LSF-LA SM, we did not further evaluate the anti-diabetic effect of LSF-LA SM by oral route as it showed low oral bioavailability and hence would also require a higher dose. Contrary to this, LSF-LA PLM formulation upon oral administration showed excellent oral bioavailability of 74.86% which

may be attributed to protection of ester bond in GIT and reduction in its interconversion to PTX (**Figure 5.6B**). This might result due to shielding of the entrapped drug molecules from direct interaction with the surrounding healthy tissues by the nano carrier and thus protecting LSF against early activation and degradation processes. The hydrophilic part of the LSF-LA PLM that is, PEG possesses brush like architecture which renders protection to the hydrophobic part from harsh environment of GIT and also minimizes protein adsorption onto its surface.[22] Owing to these reasons, LSF-LA SM underwent much faster metabolism than LSF-LA PLM as revealed by the half-life values of LSF from these two systems (**Table 5.2**). Along with oral bioavailability, LSF-LA PLM formulation after reconstitution in aqueous medium also exhibited stability at 4 °C for 1 month making it a commercially viable and patient compliant product.

LSF-LA PLM formulation was further tested in STZ induced T1D model. The glycemic level in the DC group was significantly higher compared with the normal control group. This difference in glucose homeostasis under diabetic conditions is mostly attributed to low glucose intake by peripheral tissues and high hepatic glycogenolysis and gluconeogenesis.[23,24] Diabetic rats treated with LSF and LSF-LA conjugate formulations (LSF-LA SM and LSF-LA PLM) showed decreased fasting glucose levels, when compared with DC group. Improved glycemic levels can be the result of improved insulin secretion and increase in β cell resistance to apoptosis caused by inflammatory cytokines.[1,25] Improvement was also seen in serum insulin levels after 3 weeks of treatment with LSF and LSF-LA conjugate formulations as also previously indicated by the in *in-vitro* cell culture studies. Interestingly, LSF-LA PLM showed equivalent therapeutic efficacy by both oral and i.p routes of administration at same dose of LSF possibly because of reduction in interconversion of LSF to PTX which enhanced oral bioavailability of LSF as observed in PK studies (**Figure 5.6**). LSF and its formulations significantly reduced serum cytokines levels (**Figure 5.7A**)

which also correlated well with our in-vitro results (**Figure 5.5**). Liver plays a vital role in regulating glucose levels in physiological and pathological states such as T1D.[26] Moreover, T1D is also associated with oxidative stress leading to liver injury which could be assessed by confirming the elevated levels of serum ALT and AST.[27,28] Treatment with LSF and LSF-LA PLM/SM reduced the levels of serum ALT and AST in comparison to DC and LA treated group (**Figure 5.7B**) which indicated that treatment exhibited appreciable protection from STZ induced hepatic dysfunction. Increased plasma triglyceride, high low-density lipoprotein (LDL) levels and decreased high-density lipoprotein (HDL) levels are common characteristics of dyslipidemia and can be observed in diabetic conditions due to insulin resistance-related lipolysis which results in increase in the circulating fatty acids that are taken up by the liver as an energy source.[26,29,30] LSF as a strong anti-inflammatory agent modulates stress-associated changes in lipid metabolism and suppresses serum free fatty acids.[31] Upon treatment with LSF and LSF-LA conjugate PLM/SM, serum triglycerides and total cholesterol levels were decreased while the total protein levels were increased (**Figure 5.7C and D**). Persistent hyperglycemia causes elevation in serum urea levels which is considered as one of the significant markers of renal dysfunction.[30,32,33] Serum urea levels also decreased in diabetic groups after being treated with LSF and LSF-LA PLM/SM. Few studies have examined the association between elevated serum uric acid and diabetes mellitus. The high-normal values of serum uric acid may be associated with diminished renal function in T1DM for which underlying mechanisms are not clear.[34,35] LSF and other LSF-LA conjugate groups also reduced serum uric acid levels.

Destruction of β-cells by activated T cells (CD4+ and CD8+) and macrophages of the immune system, mainly causes T1D, but unfortunately, preventing β-cell destruction has proven challenging.[36,37] To understand the protection rendered by any anti-diabetic treatment to β-cells, measurement of β-cell function along with assessment of T cell infiltration is

required. CD4+ T cells are probably responsible for stimulation of islet-resident macrophages, and for activation and propagation of CD8+ T cells which mainly infiltrate the islets of pancreas.[38] These T cells also stimulate cytokines production which further catalyzes the differentiation of native Th cells leading to overall β-cell destruction.[39-41] To assess therapeutic potential of LSF-LA PLM in immunomodulation, we first confirmed the role of LSF-LA PLM formulation in proliferation and activation of PBMCs wherein, LSF-LA PLM demonstrated significant reduction in proliferation of PBMCs and their activation. Diminished PBMCs activation was confirmed by measurement of cytokines production which showed significant decrease in the presence of LSF-LA PLM (**Figure 5.5D**). Literature shows that LSF is an inhibitor of IL-12 signaling and it inactivates functions of IL-12 in T cells as well as in macrophages. IL-12 is one of the major immunoregulatory cytokines that promotes Th1 cell differentiation, cell-mediated immune responses and induces proinflammatory cytokine production.[42,43] Further, presence of CD4+ and CD8+ T cells was confirmed in PD studies by immunohistochemical analysis of rat pancreatic sections after 3 weeks of treatment. CD4+ and CD8+ T cells were prominent in case of diabetic animals (**Figure 5.8**) while, upon treatment with LSF-LA PLM, T cells levels were significantly decreased which was possibly due to the immunomodulatory action of the drug. Similar observation was also made earlier in cell culture studies wherein, LSF prevented cell death in the presence of cytokines (**Figure 5.5E**) and prevented PBMC proliferation. Overall, this study presents the first report on a biodegradable polymeric micellar formulation of LSF that provides excellent oral bioavailability and efficacy of LSF in diabetic animals.

5. Conclusion

In this study, we demonstrated the first facile biodegradable polymeric micellar formulation of LSF that rendered excellent oral bioavailability to LSF by reducing its metabolism. Firstly, LSF-LA PLM was prepared using *in house* synthesized mPEG-b-P(CB-

co-LA) polymer and the formulation was optimized. Optimized formulation was found to be stable during storage and in different simulated biological fluids as well as in rat plasma. Further, LSF-LA PLM improved insulin secretion capability of insulinoma cells; suppressed PBMCs proliferation and exhibited enhanced cellular uptake which confirmed that there was no compromise in the potency of native LSF due to formulation development. LSF-LA PLM showed similar hypoglycemic activity by both IP and oral routes in STZ induced T1D rat model. Protection of β-cells was evident in histology of pancreatic sections after 3 weeks of treatment with LSF-LA PLM formulation which was confirmed by CD4+ and CD8+ staining of pancreata demonstrating significant reduction in T-cell population. In nutshell, our results have set the ground for a number of potential clinical applications of LSF by oral route using LSF conjugate polymeric nanoformulation.

Bibliography

1. Italiya, K. S.; Mazumdar, S.; Sharma, S.; Chitkara, D.; Mahato, R. I.; Mittal, A. Self-assembling lisofylline-fatty acid conjugate for effective treatment of diabetes mellitus. *Nanomed: NBM* **2019,** *15*, (1), 175-187.
2. Chitkara, D.; Mittal, A.; Behrman, S. W.; Kumar, N.; Mahato, R. I. Self-assembling, amphiphilic polymer–gemcitabine conjugate shows enhanced antitumor efficacy against human pancreatic adenocarcinoma. *Bioconjugate chemistry* **2013,** *24*, (7), 1161-1173.
3. Chitkara, D.; Singh, S.; Kumar, V.; Danquah, M.; Behrman, S. W.; Kumar, N.; Mahato, R. I. Micellar delivery of cyclopamine and gefitinib for treating pancreatic cancer. *Mol Pharm.* **2012,** *9*, (8), 2350-2357.
4. Danquah, M.; Fujiwara, T.; Mahato, R. I. Self-assembling methoxypoly (ethylene glycol)-b-poly (carbonate-co-L-lactide) block copolymers for drug delivery. *Biomaterials* **2010,** *31*, (8), 2358-2370.
5. Chakraborty, S.; Chakraborty, A.; Saha, S. K. Tuning of physico-chemical characteristics of charged micelles by controlling head group interactions via hydrophobically and sterically modified counter ions. *RSC Adv.* **2014,** *4*, (61), 32579-32587.
6. Eismin, R. J.; Munusamy, E.; Kegel, L. L.; Hogan, D. E.; Maier, R. M.; Schwartz, S. D.; Pemberton, J. E. Evolution of aggregate structure in solutions of anionic monorhamnolipids: Experimental and computational results. *Langmuir* **2017,** *33*, (30), 7412-7424.
7. Cui, P.; Macdonald, T. L.; Chen, M.; Nadler, J. L. Synthesis and biological evaluation of lisofylline (LSF) analogs as a potential treatment for Type 1 diabetes. *Bioorg. Med. Chem. Lett.* **2006,** *16*, (13), 3401-3405.
8. Quah, B. J.; Warren, H. S.; Parish, C. R. Monitoring lymphocyte proliferation in vitro and in vivo with the intracellular fluorescent dye carboxyfluorescein diacetate succinimidyl ester. *Nature protocols* **2007,** *2*, (9), 2049-2056.
9. Anselmo, A. C.; Mitragotri, S. An overview of clinical and commercial impact of drug delivery systems. *J. Control. Release* **2014,** *190*, 15-28.

10. Wen, H.; Jung, H.; Li, X. Drug delivery approaches in addressing clinical pharmacology-related issues: opportunities and challenges. *AAPS J* **2015,** *17*, (6), 1327-1340.
11. Banerjee, A.; Ibsen, K.; Brown, T.; Chen, R.; Agatemor, C.; Mitragotri, S. Ionic liquids for oral insulin delivery. *Proc Natl Acad Sci U S A.* **2018,** *115*, (28), 7296-7301.
12. Lu, Y.; Park, K. Polymeric micelles and alternative nanonized delivery vehicles for poorly soluble drugs. *Int J Pharm.* **2013,** *453*, (1), 198-214.
13. Xu, W.; Ling, P.; Zhang, T. Polymeric micelles, a promising drug delivery system to enhance bioavailability of poorly water-soluble drugs. *J Drug Deliv.* **2013,** *2013*.
14. Ahmad, Z.; Shah, A.; Siddiq, M.; Kraatz, H.-B. Polymeric micelles as drug delivery vehicles. *RSC Adv.* **2014,** *4*, (33), 17028-17038.
15. Owen, S. C.; Chan, D. P.; Shoichet, M. S. Polymeric micelle stability. *Nano today* **2012,** *7*, (1), 53-65.
16. Chen, Z.; FitzGerald, P. A.; Kobayashi, Y.; Ueno, K.; Watanabe, M.; Warr, G. G.; Atkin, R. Micelle structure of novel diblock polyethers in water and two protic ionic liquids (EAN and PAN). *Macromolecules* **2015,** *48*, (6), 1843-1851.
17. Apolinário, A.; Magoń, M.; Pessoa Jr, A.; Rangel-Yagui, C. Challenges for the Self-Assembly of Poly (Ethylene Glycol)–Poly (Lactic Acid)(PEG-PLA) into Polymersomes: Beyond the Theoretical Paradigms. *Nanomaterials* **2018,** *8*, (6), 373.
18. Date, A. A.; Hanes, J.; Ensign, L. M. Nanoparticles for oral delivery: Design, evaluation and state-of-the-art. *J. Control. Release* **2016,** *240*, 504-526.
19. Karavolos, M.; Holban, A. Nanosized drug delivery systems in gastrointestinal targeting: Interactions with microbiota. *Pharmaceuticals* **2016,** *9*, (4), 62.
20. Gilli, P.; Pretto, L.; Bertolasi, V.; Gilli, G. Predicting Hydrogen-Bond Strengths from Acid− Base Molecular Properties. The p K a Slide Rule: Toward the Solution of a Long-Lasting Problem. *Acc. Chem. Res.* **2008,** *42*, (1), 33-44.
21. Zhang, J.; Zhou, J.; Zhang, T.; Niu, Z.; Wang, J.; Guo, J.; Li, Z.; Zhang, Z. Facile fabrication of an amentoflavone-loaded micelle system for oral delivery to improve bioavailability and hypoglycemic effects in KKAy mice. *ACS Appl. Mater. Interfaces* **2019**.

22. Szymusiak, M.; Kalkowski, J.; Luo, H.; Donovan, A. J.; Zhang, P.; Liu, C.; Shang, W.; Irving, T.; Herrera-Alonso, M.; Liu, Y. Core–Shell Structure and Aggregation Number of Micelles Composed of Amphiphilic Block Copolymers and Amphiphilic Heterografted Polymer Brushes Determined by Small-Angle X-ray Scattering. *ACS Macro Lett.* **2017,** *6*, (9), 1005-1012.
23. Oliveira, G. O.; Braga, C. P.; Fernandes, A. A. H. Improvement of biochemical parameters in type 1 diabetic rats after the roots aqueous extract of yacon [Smallanthus sonchifolius (Poepp. & Endl.)] treatment. *Food Chem Toxicol.* **2013,** *59*, 256-260.
24. Petersen, M. C.; Vatner, D. F.; Shulman, G. I. Regulation of hepatic glucose metabolism in health and disease. *Nat Rev Endocrinol.* **2017,** *13*, (10), 572.
25. Yang, Z.; Chen, M.; Nadler, J. L. Lisofylline: a potential lead for the treatment of diabetes. *Biochem Pharmacol.* **2005,** *69*, (1), 1-5.
26. Mohamed, J.; Nafizah, A. N.; Zariyantey, A.; Budin, S. B. Mechanisms of diabetes-induced liver damage: the role of oxidative stress and inflammation. *Sultan Qaboos Univ Med J.* **2016,** *16*, (2), e132-e141.
27. Yu, Y. M.; Howard, C. P. Improper insulin compliance may lead to hepatomegaly and elevated hepatic enzymes in type 1 diabetic patients. *Diabetes Care* **2004,** *27*, (2), 619-620.
28. Aldahmash, B. A.; El-Nagar, D. M.; Ibrahim, K. E. Attenuation of hepatotoxicity and oxidative stress in diabetes STZ-induced type 1 by biotin in Swiss albino mice. *Saudi J Biol Sci.* **2016,** *23*, (2), 311-317.
29. Shoelson, S. E.; Lee, J.; Goldfine, A. B. Inflammation and insulin resistance. *J Clin Invest.* **2006,** *116*, (7), 1793-1801.
30. Jamshidi, M.; Ziamajidi, N.; Khodadadi, I.; Dehghan, A.; Kalantarian, G.; Abbasalipourkabir, R. The effect of insulin-loaded trimethylchitosan nanoparticles on rats with diabetes type I. *Biomed Pharmacother* **2018,** *97*, 729-735.
31. Bursten, S. L.; Federighi, D.; Wald, J.; Meengs, B.; Spickler, W.; Nudelman, E. Lisofylline causes rapid and prolonged suppression of serum levels of free fatty acids. *J Pharmacol Exp Ther.* **1998,** *284*, (1), 337-345.

32. Saeed, M. K.; Deng, Y.; Dai, R. Attenuation of biochemical parameters in streptozotocin-induced diabetic rats by oral administration of extracts and fractions of Cephalotaxus sinensis. *J Clin Biochem Nutr.* **2008,** *42*, (1), 21-28.

33. Jaiswal, Y.; Tatke, P.; Gabhe, S.; Vaidya, A. Antidiabetic activity of extracts of Anacardium occidentale Linn. leaves on n-streptozotocin diabetic rats. *J Tradit Complement Med.* **2017,** *7*, (4), 421-427.

34. Rosolowsky, E. T.; Ficociello, L. H.; Maselli, N. J.; Niewczas, M. A.; Binns, A. L.; Roshan, B.; Warram, J. H.; Krolewski, A. S. High-normal serum uric acid is associated with impaired glomerular filtration rate in nonproteinuric patients with type 1 diabetes. *Clin J Am Soc Nephrol.* **2008,** *3*, (3), 706-713.

35. Bandaru, P.; Shankar, A. Association between serum uric acid levels and diabetes mellitus. *Int J Endocrinol.* **2011,** *2011*.

36. Walker, L. S.; von Herrath, M. CD4 T cell differentiation in type 1 diabetes. *Clin. Exp. Immunol.* **2016,** *183*, (1), 16-29.

37. Phillips, J. M.; Parish, N. M.; Raine, T.; Bland, C.; Sawyer, Y.; De La Peña, H.; Cooke, A. Type 1 diabetes development requires both CD4+ and CD8+ T cells and can be reversed by non-depleting antibodies targeting both T cell populations. *Rev Diabet Stud.* **2009,** *6*, (2), 97-103.

38. Burrack, A. L.; Martinov, T.; Fife, B. T. T cell-mediated beta cell destruction: autoimmunity and alloimmunity in the context of type 1 diabetes. *Front Endocrinol* **2017,** *8*, 343.

39. Espinosa-Carrasco, G.; Le Saout, C.; Fontanaud, P.; Stratmann, T.; Mollard, P.; Schaeffer, M.; Hernandez, J. CD4+ T helper cells play a key role in maintaining diabetogenic CD8+ T cell function in the pancreas. *Front Immunol.* **2018,** *8*, 2001.

40. Davidson, T. S.; Longnecker, D. S.; Hickey, W. F. An experimental model of autoimmune pancreatitis in the rat. *Am J Pathol.* **2005,** *166*, (3), 729-736.

41. Tiittanen, M.; Huupponen, J. T.; Knip, M.; Vaarala, O. Insulin treatment in patients with type 1 diabetes induces upregulation of regulatory T-cell markers in peripheral blood mononuclear cells stimulated with insulin in vitro. *Diabetes* **2006,** *55*, (12), 3446-3454.

42. Yang, Z.; Chen, M.; FialkowI, L. B.; Ellett, J. D.; Wu, R.; Nadler, J. L. Inhibition of STAT4 activation by lisofylline is associated with the protection of autoimmune diabetes. *Ann N Y Acad Sci.* **2003,** *1005*, (1), 409-411.

43. Yang, Z.; Chen, M.; Ellett, J. D.; Fialkow, L. B.; Carter, J. D.; Nadler, J. L. The novel anti-inflammatory agent lisofylline prevents autoimmune diabetic recurrence after islet transplantation1. *Transplantation* **2004,** *77*, (1), 55-60.

This document was created with the Win2PDF “print to PDF” printer available at
http://www.win2pdf.com

This version of Win2PDF 10 is for evaluation and non-commercial use only.

This page will not be added after purchasing Win2PDF.

http://www.win2pdf.com/purchase/